Army Research Laboratory

Failure Fronts in Brittle Materials and Their Morphological Instabilities

by Michael A. Grinfeld, Scott E. Schoenfeld, and Tim W. Wright

ARL-TR-3660 September 2005

NOTICES

Disclaimers

Army Research Laboratory
Aberdeen Proving Ground, MD 21005-5066

ARL-TR-3660 **September 2005**

Failure Fronts in Brittle Materials and Their Morphological Instabilities

Michael A. Grinfeld, Scott E. Schoenfeld, and Tim W. Wright
Weapons and Materials Research Directorate, ARL

REPORT DOCUMENTATION PAGE	*Form Approved* *OMB No. 0704-0188*

1. REPORT DATE *(DD-MM-YYYY)*	2. REPORT TYPE	3. DATES COVERED (From - To)
September 2005	Final	1 October 2004–30 August 2005

4. TITLE AND SUBTITLE	
Failure Fronts in Brittle Materials and Their Morphological Instabilities	5a. CONTRACT NUMBER
	5b. GRANT NUMBER
	5c. PROGRAM ELEMENT NUMBER

6. AUTHOR(S)	
Michael A. Grinfeld, Scott E. Schoenfeld, and Tim W. Wright	5d. PROJECT NUMBER AH84
	5e. TASK NUMBER
	5f. WORK UNIT NUMBER

7. PERFORMING ORGANIZATION NAME(S) AND ADDRESS(ES)	8. PERFORMING ORGANIZATION REPORT NUMBER
U.S. Army Research Laboratory ATTN: AMSRD-ARL-WM-TD Aberdeen Proving Ground, MD 21005-5066	ARL-TR-3660

9. SPONSORING/MONITORING AGENCY NAME(S) AND ADDRESS(ES)	10. SPONSOR/MONITOR'S ACRONYM(S)
	11. SPONSOR/MONITOR'S REPORT NUMBER(S)

12. DISTRIBUTION/AVAILABILITY STATEMENT

Approved for public release; distribution is unlimited.

13. SUPPLEMENTARY NOTES

14. ABSTRACT

This report outlines the results of the effort to suggest a theoretical method of describing failure fronts in glasses and ceramics. There are various observations and experiments showing that in addition to standard shock-wave fronts, which propagate with transonic velocities, other much slower wave fronts can propagate within glass or ceramic substances undergoing intensive damage. These moving fronts propagate into intact substance, leaving intensively damaged substance behind them. They have been called failure waves. In this report, we model them as sharp interfaces separating two states—the intact and comminuted states. The approach is based on an analogy between failure fronts and fronts of slow combustion. Two main results are announced. One of them concerns the speed of a failure wave driven by oblique impact of a brittle target, and the other establishes a criterion for morphological instability of failure fronts.

15. SUBJECT TERMS

ceramic armor, brittle fracture, failure waves, morphological instability

16. SECURITY CLASSIFICATION OF:			17. LIMITATION OF ABSTRACT	18. NUMBER OF PAGES	19a. NAME OF RESPONSIBLE PERSON Michael A. Grinfeld
a. REPORT UNCLASSIFIED	b. ABSTRACT UNCLASSIFIED	c. THIS PAGE UNCLASSIFIED	UL	16	19b. TELEPHONE NUMBER (*Include area code*) 410-306-0793

Standard Form 298 (Rev. 8/98)
Prescribed by ANSI Std. Z39.18

Contents

List of Figures

1. Introduction

Extensive experiments with glasses and brittle ceramic materials made by different groups in Britain, Russia, and the United States in the 1990s (*1–8*) proved that failure waves exist. This conclusion is backed by other observations in geomechanics and engineering (*9–12)*.

The problem of failure waves demands significant progress of the relevant experiment (theory and numerical modeling). These three pillars grow simultaneously and in close interaction with each other. The experimenters find an analogy of such waves with solid-solid phase transformation fronts (*13)* or with fronts of slow combustion (*14*). These two analogies are not antagonistic. Modeling of both phenomena includes changes in the thermodynamic potentials of the solid states involved. Although damage is definitely not a solid/solid phase transformation, both problems have the same roots—it is the minimization of accumulated energy by big changes in the microstructure. For us, the analogy with combustion looks somewhat more relevant and appealing.

Our model is based on the analogy with the simplified theory of slow combustion. In the theory of slow wave with phase transformations, such an approach was quite successfully applied about two decades ago in geophysics and celestial physics (*15*) and in low-temperature physics (*16*). Certain difficulties of the simplified theory of phase transformation waves have been discussed in Grinfeld (*17*) and Glimm (*18*). The discussion given there is equally relevant for modeling of failure waves. According to the simplified theory, the internal wave "structure" of the wave front is ignored, and the failure front is treated as a mathematical surface. (Relevant discussions can be found in the classical monographs in Landau and Lifshitz [*19*] and Courant and Friedrichs [*20*].)

2. The Main Idea of the Model

To justify the main idea of the energetic approach, let us consider an elementary spring-like system like that shown in figure 1. The right edge of the rod is fixed. The left edge is under the action of an axial load P. The load is large enough to cause a considerable damage in the rod. The rod is divided by the failure front F into the intact domain, shown in white, and the damaged domain, shown in black. For the sake of simplicity, we assume that the intact substance has the Young's modulus E_i, whereas the weaker damaged substance has the Young's modulus $E_d < E_i$. The total energy of the model system is assumed to be equal to

$$E_{total} = \Delta P + \left(E_d \varepsilon_d^2 / 2 + e_b \right) x + E_i \varepsilon_i^2 \left(L - x \right) / 2 \, , \tag{1}$$

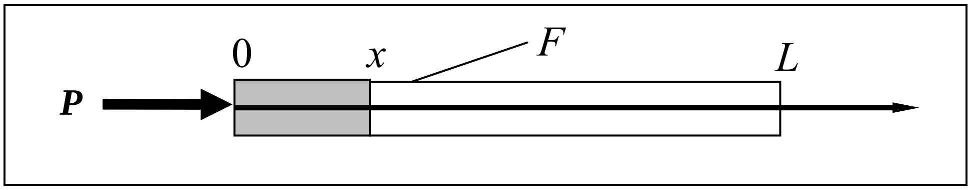

Figure 1. The energy balance for a damaged spring.

where Δ is the displacement of the left end of the rod, ε_i and ε_d are the deformations in the two domains of the combined rod, and e_b is the energy of the broken bonds per unit length. In the quasistatic evolution, we obviously get the two following equations:

$$\Delta = \varepsilon_i x + \varepsilon_d \left(L - x\right), \tag{2}$$

and

$$P = E_d \varepsilon_d = E_i \varepsilon_i . \tag{3}$$

Using the last two equations, we can rewrite the total energy of the system as follows:

$$E_{total} = \left[e_b - \left(E_d^{-1} - E_i^{-1}\right) P^2/2\right] x + P^2 L/2E_i . \tag{4}$$

The last formula implies that at a sufficiently large load, P, such that $\left(E_d^{-1} - E_i^{-1}\right) P^2 > 2e_b$, the growth of the length x of the damaged zone becomes energetically favorable.

3. Formal Statement of the Problem

We limit our study with two-dimensional propagation and consider an initially resting uniform half plane x $\geq$ 0 experiencing an impact at $x = 0$ by the oblique force P (figure 2).

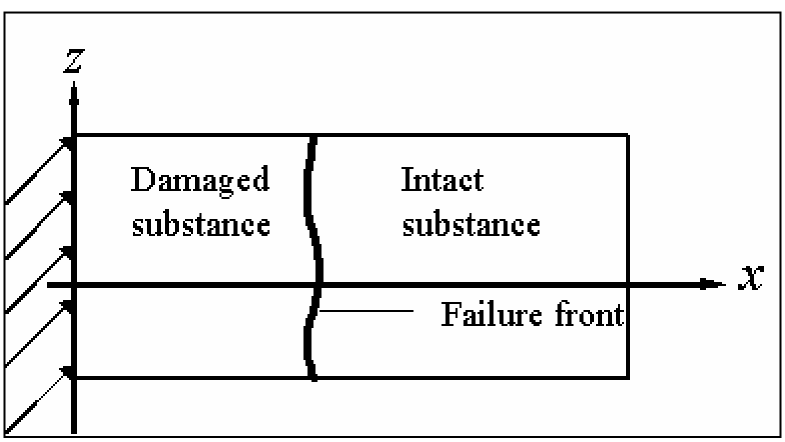

Figure 2. Oblique impact of a brittle substance.

Within each of the domains, the energy densities e_{int} and e_{dam} per unit mass of the intact and damaged states, respectively, are given by the following formulas:

$$\rho e_{int}(u_{m,n}) = (1/2)c_{int}^{ijkl}u_{i,j}u_{k,l}\,, \tag{5}$$

and

$$\rho e_{dam}(u_{m,n}) = (1/2)c_{dam}^{ijkl}u_{i,j}u_{k,l} + q_b\,, \tag{6}$$

where $u_{m,n}$ is the displacement gradients, c_{int}^{ijkl} and c_{dam}^{ijkl} are the elasticity tensors of the two states, and ρ is the original mass density ($a_{,i}$ is the symbol of differentiation with respect to the spatial coordinates x^i). Limiting ourselves with the approximation of linear elasticity, we ignore all effects of mass density change. The positive constant q_b takes into account the energy required to produce various defects (interfaces, vacancies, shear bands, holes, etc.) distributed within unit mass of the bulk of damaged substance. This term is analogous to the constant used in the theory of slow combustion, which takes into account the energy release/consumption due to chemical reactions. (See Grinfeld and Wright [*21*] for a detailed discussion of the model.)

In addition to appropriate initial and (external) boundary conditions, the master system includes the bulk equilibrium equation within each of the bulk domains (equation 7), the displacement continuity equation across the failure front (equation 8), and the traction continuity across the failure front (equation 9).

$$\frac{\partial p^{ji}}{\partial x^j} = 0\,, \tag{7}$$

$$\left[u^i\right]_-^+ n_j = 0\,, \tag{8}$$

$$\left[p^{ji}\right]_-^+ n_j = 0\,, \tag{9}$$

where $p^{ji} = \rho\partial e(u_{m,n})/\partial u_{i,j}$ is the stress tensor and n_i is the unit normal to the failure front.

The last equation (equation 10) across the failure front describes the kinetics of failure as follows:

$$c = -K\left[\mu_{.k}^{j.}\right]_-^+ n_j n^k\,, \tag{10}$$

where c is the velocity of the failure front, the tensor $\mu_{.k}^{j.}$ is defined as $\mu_{.k}^{j.} = e\delta_k^j - \rho^{-1}p^{ji}\left(\delta_{ik} + u_{i,k}\right)$—it plays the same role as the scalar Gibbs chemical potential μ of a liquid substance—and K is a positive (kinetic) constant or function with dimension [*velocity*]$^{-1}$. We assume explicitly that the displacements and traction remain continuous across the interface. This is not the only reasonable option. Another reasonable option, especially when dealing with pulverized states, would be the model of a friction-free interface with discontinuous displacements. In this case, the last kinetic, constitutive equation (equation 10) should be modified as well (a similar system was analyzed in Parshin [*16*] and Grinfeld [*17*] in the context of phase transformations).

The system (equations 7–10) allows piecewise linear solutions of the following forms:

$$u_+^i(x,z,t) = d_+^i t + a_+^i z \text{ at } x \geq ct \ , \tag{11}$$

and

$$u_-^i(x,z,t) = d_-^i t + a_-^i z \text{ at } x \leq ct \ , \tag{12}$$

where $d_\pm^i$, $a_\pm^i$, and c are certain constants. The sign ± marks the quantities related to the intact (damaged) state. The constant c gives the speed of the failure front across which the displacement gradients $a_\pm^i$ suffer the finite discontinuities. The solution just mentioned allows considering the quasistatic problem oblique impact (loading) when the applied force has the following components:

$$p_\pm^{xx} = \pi \ , \tag{13}$$

and

$$p_\pm^{zx} = \tau \ . \tag{14}$$

In this case, the system (equations 7–10) leads to the following formula of the velocity of the failure front:

$$\frac{\rho}{K} c = \frac{\pi^2}{2}\left(\frac{1}{\lambda_- + 2\mu_-} - \frac{1}{\lambda_+ + 2\mu_+}\right) + \frac{\tau^2}{2}\left(\frac{1}{\mu_-} - \frac{1}{\mu_+}\right) - q_b \ . \tag{15}$$

4. Morphological Instability of the Failure Front

In order to explore morphological stability of the piecewise linear solution, we present the elastic displacement $u_\pm^i(x,z,t)$ and the speed of the interface $c(z,t)$ in the following forms:

$$u_\pm^i(x,z,t) = u_\pm^{\circ i}(x,t) + \tilde{u}_\pm^i(x,z,t) \ , \tag{16}$$

and

$$c(z,t) = c^\circ + \tilde{c}\ (z,t) \ , \tag{17}$$

where $\tilde{u}_\pm^i(x,z,t)$ and $\tilde{c}(z,t)$ are small disturbances. These equations should be substituted in the bulk equations and in the boundary conditions (equations 7–10), which should then be linearized with respect to the small disturbances. We then look for the solutions of the linearized system in the following forms (k is the in-plane wave-number and η is the rate of growth):

$$\tilde{u}^i_{\pm}(x,z,t) = W^i_{\pm}\left(x - c^{\circ}t\right)e^{ikz+\eta t}, \tag{18}$$

and

$$\tilde{c}(z,t) = Se^{ikz+\eta t}, \tag{19}$$

where the functions $W^i_{\pm}(X)$ should decay exponentially at $X \to \pm\infty$. The dispersion equation for η is too lengthy to be presented here. It becomes relatively compact and instructive in the limit of an incompressible damaged state ($\nu_- = 1/2$) and $\nu_+ = 1/3$ $\left(\nu_{\pm} = \lambda_{\pm}/2\left(\lambda_{\pm} + \mu_{\pm}\right)\right)$ when it reads as follows:

$$\frac{\rho}{8Kk}\eta = \frac{\mu_+\left(\mu_+^2 - \mu_-^2\right)}{5\mu_-^2 + 8\mu_-\mu_+ + 3\mu_+^2} - 4\frac{\mathrm{T}^2}{\Pi^2}\frac{\mu_+\left(\mu_+ - \mu_-\right)^2}{\mu_-}\frac{4\mu_- + 3\mu_+}{5\mu_-^2 + 8\mu_-\mu_+ + 3\mu_+^2}. \tag{20}$$

The wave front is morphologically unstable if the linearized master equation has solutions of the previous form and with the rate η corresponding to exponential growth in time. The last formula shows that shear stresses T play a stabilizing role (similar to the case of morphological instabilities of solid-solid phase interfaces [*17*]). In addition, at $\mathrm{T} = 0$, the failure front is morphologically unstable in the most interesting case when the shear modulus μ_- of the damaged state is less than the shear modulus μ_+ of the intact state. Speaking very schematically, the instability has a simple, physical meaning. It means that penetration of fingers of damaged material into intact material is the fastest way of releasing accumulated elastic energy from the system.

The morphological failure-front instability has the potential to explain appearance of fingering cracks on disintegration fronts in Prince Rupert drops reliably documented in experiments of Chandrasekar and Chaudhri (4). This interpretation, however, requires further (numerical) studies of deeply nonlinear stage of the instability. Another appealing possibility of the instability applications is to the failure-front waviness that was detected in the numerical modeling of Resnyansky et al. (*22*). These authors use a formally different, but conceptually close, model. Appearance of the waviness in their simulations could be not a numerical artifact but a manifestation of the instability discussed here.

In conclusion, we have presented a simple model for a failure front based on an analogy with slow combustion and a formula for the failure wave generated by oblique impact on brittle material. We then demonstrated that under rather general assumptions, the flat failure front is morphologically unstable. The last conclusion shows an additional analogy between failure fronts and slow combustion fronts (but, of course, the mechanisms of destabilization are totally different). The morphological instability discussed here may shed some light on the appearance of corrugations on failure fronts and crack bifurcations as observed in experiments on static indentation of brittle materials, the appearance of radial cracks in dynamic experiments with penetration of projectiles through brittle materials, the appearance of corrugations on the disintegration fronts in Prince Ruppert drops (*4*), and the appearance of failure front waviness detected in numerical simulations (*22*).

5. References

1. Kanel G. I.; Molodets, A. M.; Dremin, A. N. *Combust. Explos. Shock Waves* **1977**, *13*, 772.

2. Brar, N. S.; Bless, S. J.; Rozenberg, Z. *J. Appl. Phys*. **1991**, *59*, 3396.

3. Bless, S. J.; Brar, N. S.; Kanel, G.; Rozenberg, Z. *J. Amer. Ceramic Soc*. **1992**, *75*, 1002.

4. Chandrasekar, S.; Chaudhri, M. M. *Phil. Mag. B* **1994**, *70* (6), 1195–1218.

5. Dandekar, D. P.; Beaulieu, P. A. *Metallurgical and Materials Applications of Shock-Wave and High-Strain-Rate Phenomenon*; Murr, L. E., Staudhammer, K. P., Meyers, M. A., Eds.; Elsevier Science: New York, 1995; pp 211–218.

6. Bourne, N.; Rosenberg, Z.; Field, J. E. *J. Appl. Phys*. **1995**, *78*, 3736.

7. Bourne, N. K.; Forde, L.; Field, J. E. Speed Photography and Photonics–1996; Paisley, D. L. Ed.; *Proc. SPIE 2869* **1997**, 626.

8. Bourne, N.; Millett, J.; Rosenberg, Z. *J. Appl. Phys*. **1997**, *81*, 6670.

9. Grigoryan, S. S. *PMM* **1967**, *31*, 667.

10. Slepyan, L. I. *MTT* **1977**, *1*, 181.

11. Chaudhri, M. M. *Phil. Mag. Lett*. **1998**, *78* (2), 153–158.

12. Grady, D. E. *Mech. Mat*. **1998**, *29*, 181.

13. Clifton, R. J. *Appl Mech. Rev*. **1993**, *46*, 540.

14. Kanel, G. I.; Bogatch, A. A.; Razorenov, S. V.; Chen, Z. *J. Appl. Phys*. **2002,** *92*, 5045.

15. Grinfeld, M. A. *Dokl. AN SSSR* **1982,** *262*, 1339.

16. Parshin, A. Ya. *Low Temperature Physics*; Borovik-Romanov, A. S., Ed.; Mir, Moscow, 1985.

17. Grinfeld, M. A. *Thermodynamic Methods in the Theory of Heterogeneous Systems*; Longman: Sussex, 1991.

18. Glimm, J. *Lecture Notes in Phys*. **1989**, *344*, 177.

19. Landau, L. D.; Lifshitz, E. M. *Fluid Mechanics*; Pergamon Press: New York, 1987.

20. Courant, R.; Friedrichs, K. O. *Supersonic Flow and Shock Waves*; Springer-Verlag: New York, 1948.

21. Grinfeld, M. A.; Wright, T. W. *Metall. Mater. Trans. A* ***2004***, *35* (9), 2651–2661.

22. Resnyansky, A. D.; Romensky, E. I.; Bourne, N. K. *Journal Appl. Phys. 93* **2003**, 1537.

NO. OF COPIES	ORGANIZATION
1 (PDF ONLY)	DEFENSE TECHNICAL INFORMATION CTR DTIC OCA 8725 JOHN J KINGMAN RD STE 0944 FORT BELVOIR VA 22060-6218
1	US ARMY RSRCH DEV & ENGRG CMD SYSTEMS OF SYSTEMS INTEGRATION AMSRD SS T 6000 6TH ST STE 100 FORT BELVOIR VA 22060-5608
1	INST FOR ADVNCD TCHNLGY THE UNIV OF TEXAS AT AUSTIN 3925 W BRAKER LN AUSTIN TX 78759-5316
1	DIRECTOR US ARMY RESEARCH LAB IMNE ALC IMS 2800 POWDER MILL RD ADELPHI MD 20783-1197
3	DIRECTOR US ARMY RESEARCH LAB AMSRD ARL CI OK TL 2800 POWDER MILL RD ADELPHI MD 20783-1197
3	DIRECTOR US ARMY RESEARCH LAB AMSRD ARL CS IS T 2800 POWDER MILL RD ADELPHI MD 20783-1197
	ABERDEEN PROVING GROUND
1	DIR USARL AMSRD ARL CI OK TP (BLDG 4600)

NO. OF COPIES	ORGANIZATION
1	DIRECTOR US ARMY RESEARCH LAB AMSRD ARL RO EN A RAJENDRAN RESEARCH TRIANGLE PARK (ARO) DURHAM NC 27703
13	JOHNS HOPKINS UNIVERSITY DEPT OF MECHL ENGRG F ZHOU K VOLOKH T HUFNAGEL Z HAITAO E MA J-F MOLINARI K J HEMKER K TRAMESH Q WEI B PALIWAL G WENG S C DANFORTH W TIM LATROBE 122 3400 N CHARLES ST BALTIMORE MD 21218

ABERDEEN PROVING GROUND

NO. OF COPIES	ORGANIZATION
51	DIR USARL AMSRD ARL CI HC D GROVE AMSRD ARL WM M GREENFIELD T WRIGHT AMSRD ARL WM M J BEATTY J MCCAULEY AMSRD ARL WM MB K CHO R DOWDING L KECSKES M STAKER J SWAB R WOODMAN AMSRD ARL WM MC R ADLER J LASALVIA AMSRD ARL WM MD J ADAMS J CAMPBELL B CHEESEMAN E CHIN K DOHERTY C FOUNTZOULAS G GAZONAS S GHIORSE G GILDE P HUANG P PATEL W ROY T SANO C YEN AMSRD ARL WM TA M BURKINS W GOOCH V HERNANDEZ C HOPPEL E HORWATH D KLEPONIS C KRAUTHAUSER B LEAVY D MACKENZIE AMSRD ARL WM TC R COATES M FERMEN COKER L MAGNESS B SCHUSTER C WILLIAMS AMSRD ARL WM TD D CASEM D DANDEKAR K IYER H MEYER M RAFTENBERG E RAPACKI M SCHEIDLER S SCHOENFELD S SEGLETES T WEERASOORIYA